To Enabling Plant-like Movement Capabilities in Continuum Arms

Enrico Donato
The BioRobotics Institute &
Dept. of Excell. in Robotics and AI
Scuola Superiore Sant'Anna
Pisa, Italy
e.donato@santannapisa.it

Yasmin Tauqeer Ansari
The BioRobotics Institute &
Dept. of Excell. in Robotics and AI
Scuola Superiore Sant'Anna
Pisa, Italy
y.ansari@santannapisa.it

Cecilia Laschi
Dept. of Mechanical Engineering
National University of Singapore
Singapore
mpeclc@nus.edu.sg

Egidio Falotico
The BioRobotics Institute &
Dept. of Excell. in Robotics and AI
Scuola Superiore Sant'Anna
Pisa, Italy
e.falotico@santannapisa.it

***Abstract*—Enabling reaching capabilities in highly redundant continuum soft arms is an active area of research. So far, it has been heavily addressed through the brain-inspired notion of internal models, where sensory-motor spaces are correlated through learning-based computational frameworks. However, this work investigates an innovative source of bio-inspiration, i.e., plants, which can interestingly move towards a desired external stimulus despite the lack of a central nervous system, thereby, opening avenues to the development of a new generation of distributed control strategies for continuum arms. In particular, reaching is achieved through a combination of distributed sensing and curvature regulation. This work is a first translation of moving-by-growing mechanisms in plants intended to endow continuum and soft robotic arms with a novel repertoire of motions that can be exploited to efficiently navigate highly unstructured environments.**

***Index Terms*—Bio-inspired Control, Model free, Proprioception, Reaching, Continuum Arm**

I. Introduction

It is a common misconception that the crucial difference between animals and plants lies in the lack of movements in the latter. However, plants have evolved movement strategies, based on growth, that they exploit to move from one point to another. In comparison to their roaming counterparts, plant growth occurs at timescale that is significantly elapsed, resulting in their seemingly sessile nature. In this regard, digital time-lapse recording systems have demonstrated that plants move both with purpose and with intent, with exceptional capabilities to negotiate with a wide range of terrains and external disturbances. These desirable characteristics have inspired a new generation of robotic arms made up of soft material [1], [2], from which we focus on a continuum soft arm.

The successful application of these machines will rely on control architectures that adapt to dynamically changing situations. This work exploits an untapped source of bio-inspiration to address this challenge, i.e., the impressive feat of plant adaptation to surrounding environments which arises despite the lack of a central nervous system, thereby, opening avenues for a novel control paradigm for soft robot arms.

This work was supported by the European Union's Horizon 2020 Research and Innovation Programme through GROWBOT Project under Grant 824074.

From amoung different behaviours, our work focuses on phototropism, where plants are able to grow towards/away from an external stimulus through differential bending [3], [4]. In particular, such behaviour arises from a distributed information processing system that relies on exploiting information from biosensors distributed across the plant body to decide the direction to bend towards. Furthermore, to avoid overshooting a desired external stimulus, plants dampen their curving dynamics through the application of a restoring force proportional to the current curvature, known as proprioception [5]–[8]. Taking cue from these concepts lays the foundation of a distributed controller that can enable reaching capabilities in soft arms.

Reaching tasks have already been implemented for continuum and soft robots. Such a control strategy usually requires a model to estimate the configuration of the structure given the actuation [9], [10]. A model is not easy to be obtained analytically and in closed form due to the complexity of morphology and because materials of continuum robots usually show high hysteresis [11]. Alternatively, learning algorithms can map the actuation space into the task space after huge data collection but generate a model with no semantic value [12], [13].

The central contribution of our work is to take inspiration from the above-mentioned biological principles to develop a novel distributed controller. Specifically, it comprises of low-level restoring functionalities combined in a bottom-up manner to generate the complex capability of reaching. The controller is tested on a 9-DoF modular cable-driven continuum arm for reaching multiple set-points in space. Results demonstrate that including the bio-inspired notion of proprioception allows for reducing oscillations around the target.

II. Materials and Methods

A. Robotic Platform

The proposed controller is tested on a novel modular continuum arm [14], shown in Fig.1. It takes inspiration from plants to decrease flexural stiffness and tapering diameter from the base toward the tip, thereby, enabling it to self-support its weight and stand upright. Note that this capability is also facilitated by the hollow structure of the modules, in order to reduce weight of the overall system. In total, the robot has six

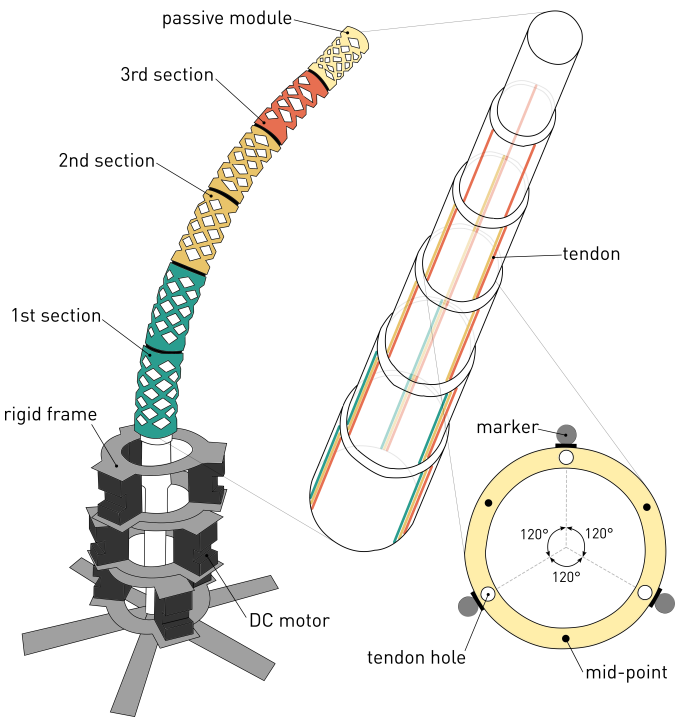

Fig. 1: A rigid frame anchors the continuum arm and encases the nine servo motors to pull tendons. The four sections and respective tendons are identified on the robot. Cross-section and markers position for a single module are shown.

modules arranged in series, divided into four sections.

(a) The first three sections are made up of a pair of modules in series, each of which comprises of longitudinally arranged tendons spaced 120 degrees apart. This arrangement allows for the section to exhibit omnidirectional bending, provided differential input. Note that the triad of tendons are independently activated by motors (Dynamixel XM430-W210-R), which also provide feedback in position, velocity, and torque. A rigid 3D-printed frame encases the motors and allows rigidly anchoring the robot, such that the tendons are taut.

(b) The last module which is kept passive.

In regards to the sensing, vision-based tracking system (Vicon) has been employed to provide environmental feedback, i.e., 3D position in Cartesian space. In particular, three retro-reflective markers are distributed at the tip of each modular section, placed directly in front of actuators. The three markers' positions belonging to the same cross-section of a module are used to compute its pose in space. Therefore, the robot's configuration is the set of all sections' poses. The arrangement of the markers in this manner serves two purposes: (i) for the functioning of the controller, and; (ii) to monitor the arm configuration through progressive motion towards a target.

B. Control Architecture

Distributed control architectures comprise of task-achieving modules, known as behaviours, combined in a bottom-up manner.

It is well-known that a triad of radially arranged flexible actuators can generate six principal directions of bending, i.e., by activating a single tendon or activating two adjacent tendons. In the former case, a single tendon in the proximal modular section is activated, and the corresponding tendons in the remaining distal modular sections that share a common actuation route. On the other hand, the second case occurs by activating two adjacent tendons in the proximal modular section and the corresponding tendons of the remaining distal modular sections that share a common actuation route.

Based on this, we define two basic behaviours: (i) bending – agonistic tendons are contracted in order to bend the system towards a stimulus; (ii) resistance to bending – antagonistic tendons tend to bend the system in a direction opposite to (i). Note that two modalities for antagonistic tendons actuation have been considered. In the first case, the antagonists are shortened by a constant restoring length Δl_r. Alternatively, if the agonists are shortened by a pulling length Δl_r, the antagonists will bedecreased in the restoring length according to this law:

$$\Delta l_r = \alpha \Delta l_p \tag{1}$$

where $\alpha \in [0, 1]$. If $\alpha = 0$, restoring will be null. If $\alpha = 1$, the arm will not bend but shorten. The restoring law can also change proportionally to the curvature of the respective section. The curvature κ of a three-tendons module with diameter d is a function of their lengths l_1, l_2, l_3 [15]:

$$\kappa(l_1, l_2, l_3) = \frac{2\sqrt{l_1^2 + l_2^2 + l_3^2 - l_1 l_2 - l_1 l_3 - l_2 l_3}}{d(l_1 + l_2 + l_3)} \tag{2}$$

The length of the antagonistic tendons is not considered to change over time, so the restoring force will be proportional to the curvature in case no antagonistic tendons have already been shortened. For example, if l_1 is agonist, then the curvature is computed as $\kappa(l_1, \bar{l_2}, \bar{l_3})$ where $\bar{l_2}, \bar{l_3}$ are constant over time. In conclusion, the antagonists are shorten according to Eq.(1), with $\alpha = \kappa$. Examples of agonistic and antagonistic activations in different configurations are given in Fig. 2.

These two behaviours are combined in a bottom-up manner to formulate the overall controller as shown in Fig.3. In particular, provided that a target is placed within the vision-system's field-of-view, the controller aims to reduce the distance between arm's tip and the target, by bending towards that direction. To achieve this objective, a two-step loop is implemented starting from a straight configuration to reach the target.

(i) Considering one single module, six points are identified: the three related to markers (from tracking software) and their cross-section mid-points (geometrically computed). In this way, marker points are in line with a principle bending direction that arises from pulling the adjacent tendon (i.e., 0 deg, 120 deg, 240 deg), while the estimated points are along the principle direction of bending which arises from pulling two adjacent tendons (i.e., 60 deg, 180 deg, 300 deg).

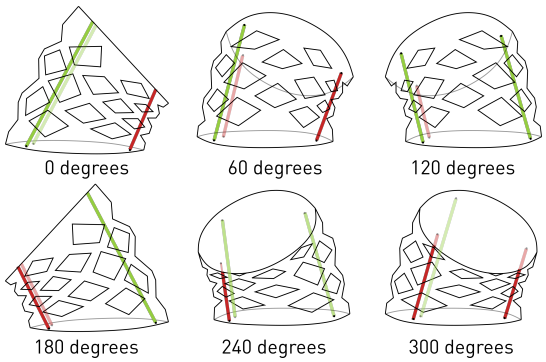

Fig. 2: The activation of a specific tendon pattern causes bending in one direction. For each combination, agonist (red) and antagonist (green) tendons can be identified. The six possible combinations of actuation that produce omnidirectional bending for a single module are shown.

(ii) The point closest to the target is identified, and a command is sent to actuators to bend in the corresponding principal bending direction.

Note that the resistance to the bend is pre-defined. The objective of the experiments is to determine whether the notion of this resistance plays a significant role in achieving the objective of successful reaching.

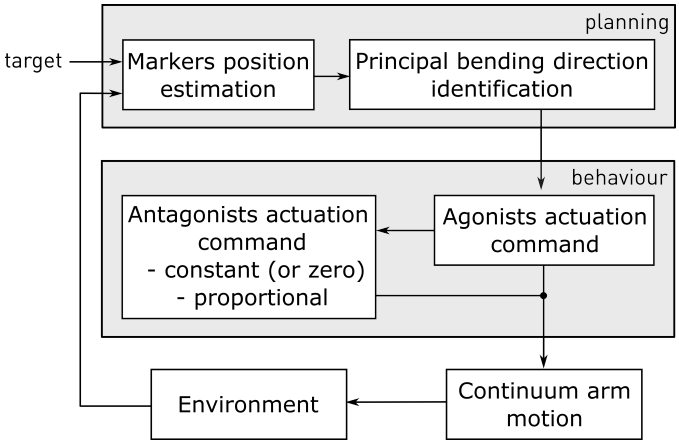

Fig. 3: Control strategy work flow.

III. Results

The six main bending directions are identified and shown in Fig.4 by activating the corresponding tendons from 0 to 4π radians in 22 steps. In general, the principal directions of bending are spaced 60 degrees apart. For each direction, it can be seen that the bending pattern remains consistent for each module. Furthermore, from the initial configuration of the robot along the positive z-axis, the robot rotates through a bending angle of approximately 55 degrees.

Interestingly, the change in the bending angle from the initial configuration toward the final configuration exhibits a linear trend. Note that the change in bending angles for each

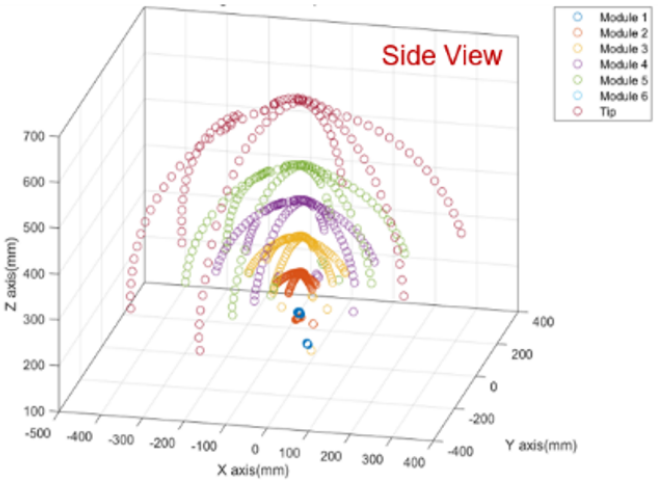

Fig. 4: The overall bending angle achieved by rotating dedicated motors. Each section is represented by a different color.

direction varies due to fabrication inconsistencies, gravitational effects and not perfect longitudinal cable arrangement.

The target position is chosen for each trial to let the robot cover its entire workspace, to demonstrate that the strategy is invariant to the target position. In particular, the target is positioned at 21 different locations out of the workspace, with different heights and angles. For each location, 3 trials were performed to statistically validate the robot's movement. Some target positions are shown in Fig. 5 with the respective closest arm configurations.

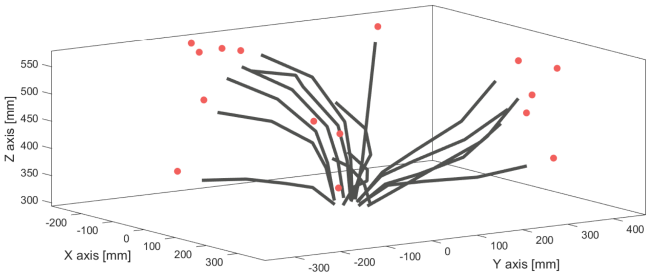

Fig. 5: Experimental workspace and closest reaching configurations of the continuum arm.

The notion of principal bending directions is used to implement the reaching strategy. A target is placed in the space and kept fixed over time. The arm is initially straight and four different restoring forces are tested, as in Tab. I.

No restoring force	Eq.(1), $\alpha = 0$
High restoring force	$\Delta l_r = 100$
Low restoring force	$\Delta l_r = 20$
Proportional restoring force	Eq.(1), $\alpha = \kappa$

TABLE I: Restoring forces applied to the robot within a trial

Results from an experimental trial are shown in Fig.6. In case no restoring force is applied, the continuum arm reaches the minimum distance from the target after 15 seconds

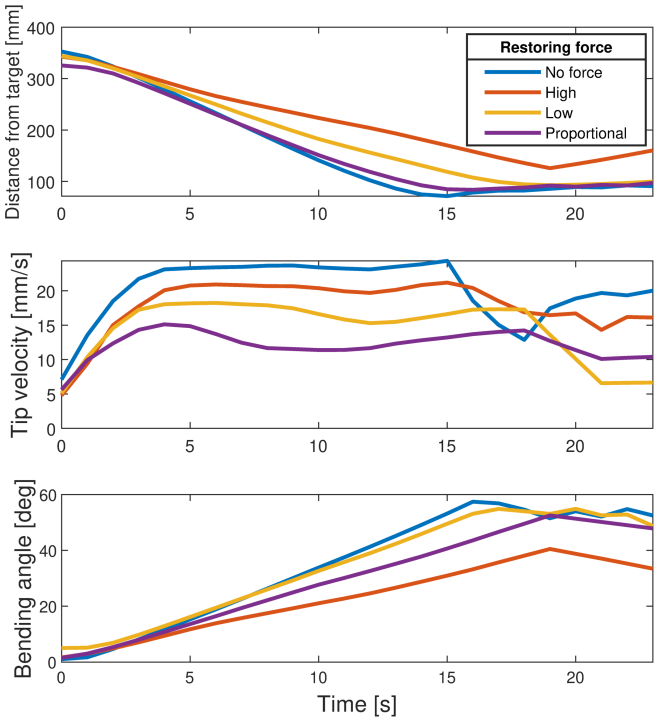

Fig. 6: For each restoring force, the distance from the target, the tip velocity and the bending angle of the continuum arm are reported in the graph.

and keeps it constant until the end of the trial. The task is successful as the distance has reached a plateau that coincides with the minimum of the curve. Despite this, it continues oscillating around its configuration as demonstrated by the tip velocity. Similar considerations holds for the bending angle.

We consider the case in which a restoring force is in action. With a constant high force, the tip never approaches the target and maintains an almost constant speed throughout the task. In addition, the bending angle is lower than in the other cases, as the restoring force is too high and does not allow for high bending of the structure. Conversely, with the constant low force, the arm reaches the closest position later than in the no-force case, but the tip moves at a lower speed.

Finally, the control with the proportional restoring force to the curvature allows the optimal configuration to be reached in the same time as in the no-force case, but with an overall tip speed that is lower than in all other cases. It therefore remains almost constant around its best configuration. In addition, the bending angle is consistent with that observed for the force-free case, used as a baseline to compare the performance of the proposed controller.

The proportional force case achieves the best performance and also guarantees the highest stability of the system compared to other strategies.

IV. Conclusion and Future Works

A plant-inspired reaching behaviour is implemented for a continuum arm. Task control is implemented without any internal model representation of the robot but only relies on sensory information. Proprioception allows the robot to get better reaching performance than in other cases. Indeed, modulating the restoring force permits the robot to reach the target with a stable configuration that minimizes the discrepancy from the tip without any oscillation.

This implementation is a proof-of-concept that exploits an external motion capture system to get the continuum arm configuration, using such information for proprioception. Further improvements of this work might include using embedded sensors to implement similar functionalities to let the robot not rely on external sensors. Alternative arrangements of tendons can be inspected to get different behaviours that could help to improve the task performance. In addition, the primitive reaching mechanism could be used to implement target tracking strategies or to observe whether it is robust against external disturbances that alter the internal structure of the robot.

References

[1] R. Bastien, A. Porat and Y. Meroz, "Towards a framework for collective behavior in growth-driven systems, based on plant-inspired allotropic pairwise interactions", *Bioinspiration & Biomimetics*, 14, 2019. DOI: 10.1088/1748-3190/ab30d3

[2] B. Mazzolai, F. Tramacere, I. Fiorello and L. Margheri, "The Bio-Engineering Approach for Plant Investigations and Growing Robots. A Mini-Review", *Frontiers on Robotics and AI*, 7, 2020. DOI: 10.3389/frobt.2020.573014

[3] D.E. Moulton, H. Oliveri and A. Goriely, "Multiscale integration of environmental stimuli in plant tropism produces complex behaviors", *PNAS*, 117(51), 2017. DOI: 10.1073/pnas.2016025117

[4] S. Gilroy, "Plant Tropisms", *Current Biology*, 18(7), 2008. DOI: 10.1016/j.cub.2008.02.033

[5] R. Bastien, S. Douady and B. Moulia, "A Unified Model of Shoot Tropism in Plants: Photo-, Gravi- and Propio-ception", *PLOS Computational Biology*, 11(2), 2014. DOI: 10.1371/journal.pcbi.1004037

[6] O. Hamant and B. Moulia, "How do plants read their own shapes?", *New Phytologist*, 212(2), pp. 333-337, 2016. DOI: 10.1111/nph.14143

[7] O.E. Jensen, "A field theory for plant tropisms", *PNAS*, 118(1), 2021. DOI: 10.1073/pnas.2023962118

[8] Y. Meroz, "Plant tropisms as a window on plant computational processes", *New Phytologist*, 229(4), 2021. DOI: 10.1111/nph.17091

[9] R. Kang, D.T. Branson, E. Guglielmino and D.G. Caldwell, "Dynamic modeling and control of an octopus inspired multiple continuum arm robot", *Computers and Mathematics with Applications*, 64, pp. 1004-1016, 2012. DOI: 10.1016/j.camwa.2012.03.018

[10] T.G. Thurthel, Y. Ansari, E. Falotico and C. Laschi, "Control Strategies for Soft Robotic Manipulators: A Survey", *Soft Robotics*, 5(2), pp. 149-163, 2018. DOI: 10.1089/soro.2017.0007

[11] F. Renda, M. Giorelli, M. Calisti, M. Cianchetti and C. Laschi, "Dynamic Model of a Multibending Soft Robot Arm Driven by Cables", *IEEE Transactions on Robotics*, 30(5), pp. 1109-2014, 2014. DOI: 10.1109/TRO.2014.2325992

[12] T.G. Thuruthel, E. Falotico, M. Manti, A. Pratesi, M. Cianchetti and C. Laschi, "Learning Closed Loop Kinematic Controllers for Continuum Manipulators in Unstructured Environments", *Soft Robotics*, 4(3), pp. 285-296, 2017. DOI: 10.1089/soro.2016.0051

[13] A. Centurelli, L. Arleo, A. Rizzo, S. Tolu, C. Laschi and E. Falotico, "Closed-Loop Dynamic Control of a Soft Manipulator Using Deep Reinforcement Learning", *IEEE Robotics and Automation Letters*, 7(2), pp. 4741-4748, 2022. DOI: 10.1109/LRA.2022.3146903

[14] F. Visesntin, G.A. Naselli and B. Mazzolai, "A New Exploration Strategy for Soft Robots Based on Proprioception", *2020 3rd IEEE RoboSoft*, pp. 816-821, 2020. DOI: 10.1109/RoboSoft48309.2020.9115976

[15] R.J. Webster III and B.A. Jones, "Design and Kinematic Modeling of Constant Curvature Continuum Robots: A Review", *The International Journal of Robotics Research*, 29(13), pp. 1661-1683, 2010. DOI: 10.1177/0278364910368147